日本海域研究，第48号，17-28ページ，2017
JAPAN SEA RESEARCH, vol.48, p.17-28, 2017

Seasonal Variability of Wave Characteristics and Related Morphological Indices on the Kaetsu Coast, Ishikawa, Japan

Trinh Chung NGUYEN[1], Masatoshi YUHI[2*] and Takuya UENO[3]

Received 23 September 2016
Accepted 1 December 2016

Abstract

This study investigates the seasonal variability of wave characteristics and related morphological indices on the Kaetsu Coast in Ishikawa, Japan based on long-term wave data observed at Kanazawa Port from 1971 to 2012. First, the seasonal variations of wave energy flux are investigated in combination with the directional distribution. Most of the incoming wave energy is concentrated in the winter season, in which high waves from the WNW, NW, and NNW direction frequently impact the coastline. Second, the characteristics of wave breaking in the near shore area, and breaker height and depth, are examined. Related morphological indices such as the closure depth and the Sunamura index are also estimated. The seasonal variations of these properties indicate common patterns, in which the values are highest in winter, medium in spring and autumn, and lowest in summer. The cumulative probability of breaker depths varies significantly from season to season. The estimated closure depth also indicates distinct seasonal changes. These results indicate that the cross-shore width of significant morphological change is substantially variable according to the time. The estimations of the Sunamura indices suggest that the shoreline is advanced during the summer, while shoreline recessions generally occur in other seasons. The transitions from shoreline recessions to shoreline advances are deduced to occur in March, and from advances to recessions in September. Third, an analysis of infragravity waves is conducted. The patterns of the daily as well as monthly variations of infragravity wave heights are similar to that of wind waves. A strong linear correlation exists between the heights of infragravity waves and wind waves.

Key Words: Kaetsu Coast, wave climate, seasonal variation, wave energy, morphological index.

I. Introduction

The ocean wave statistics play a key role in a variety of coastal projects. An accurate estimation of wave characteristics is of crucial importance, for example, in the planning of countermeasures against wave-induced coastal disasters, the design and management of ports, the utilization of wave energy, the mitigation of accelerated erosion of sandy beaches, the conservation of coastal ecosystem, and others. As a dominant external force on the coastline, the basic information on incident wave characteristics is extremely important to cope with these devastating problems.

Located on the middle north coast of Japan, the Kaetsu Coast in Ishikawa Prefecture faced to the Sea of Japan. The coastline includes approximately 75 km

[1]Division of Environmental Science and Engineering, Graduate School of Natural Science and Technology, Kanazawa University, Kakuma-Machi, Kanazawa, 920-1192 Japan
[2]Institute of Environmental Design, Faculty of Science and Engineering, Kanazawa University, Kakuma-Machi, Kanazawa, 920-1192 Japan
[3]Division of Environmental Design, Graduate School of Natural Science and Technology, Kanazawa University, Kakuma-Machi, Kanazawa, 920-1192 Japan
*Author for correspondence

alongshore stretch and has a general NNE-SW orientation (Fig. 1). The coast has experienced various problems related to wave and sediment dynamics during the last decades such as the destruction of coastal facilities by violent winter waves, the rapid and severe erosion over the most part of the alongshore stretch, the frequent occurrences of rip current accidents in summer, the reduction of coastal habitats, and others. Since the waves act as the principal driving force of sediment transport and are closely related to morphological change in many of these problems, physical understanding is needed not only for the wave characteristics themselves but also for the influence on morphological responses.

On the wave climate along the Sea of Japan coast, several studies in the last decades demonstrated that the seasonal variation of wave height and period is significant (*e.g.* Kobune *et al.*,1988; Nagai, 1997; Shimizu, 2006; Yamaguchi *et al.*, 2007; Seki *et al.*, 2011, 2012). More recently and specifically, Nguyen *et al.* (2015, 2016) conducted a detailed statistical analysis on the seasonal and long-term variability of wave characteristics at the Kaetsu Coast based on the long-term wave record at Kanazawa Port in duration 1971-2012. The results clarified the characteristics of long-term as well as seasonal variability of wave height, period, and direction at the Kaetsu Coast. The focus was, however, placed on the variation of wave properties at the offshore; the available information is limited for the wave properties in the nearshore area, and the related influence on the sediment transport and morphological changes has not been discussed yet. It is therefore desirable to extend the previous researches and further explore the seasonal variability of wave behavior in the nearshore area and to estimate the resulting morphological response to variable wave forcing.

Accordingly, this study further investigates the characteristics of wave forcing and expected morphological responses at the Kaetsu Coast based on the long-term wave data observed at Kanazawa Port in duration 1971-2012. First, as a complementary analysis to Nguyen *et al.* (2015, 2016), the monthly and seasonal variation of wave energy flux at the offshore area is investigated in combination with the directional distribution to understand the seasonal variability of the magnitude and direction of wave forcing. Second, several kinds of morphological indices that are closely related to incident wave properties are examined in order to deduce the characteristics of morphological response to the seasonally-varying wave conditions. For this purpose, the characteristics of wave breaking in the nearshore region, breaker height and depth, are examined in order to deduce the seasonal variation of the cross-shore width of surf zone where significant morphological changes occur. Moreover related morphological indices such as the closure depth and Sunamura index are estimated to discuss the seaward extent of significant morphological change and the dominant direction of cross-shore sediment movement, respectively. The occurrence probabilities and the probability of non-exceedance of these properties are then computed based on the monthly-mean values. Based on the cumulative probability of breaker depth, closure depths and the Sunamura index the seasonal variation of the width of breaker zone and the advance and recession of shoreline are discussed. Finally, the characteristics of infragravity waves (long-period waves), that is known to strongly affect the swash zone dynamics during high waves (Guza and Thornton, 1982; Masselink *et al.*, 2003), are investigated to clarify the relation with wind wave characteristics.

II. Field Site, Datasets and Method of Analysis

1) Field Site and Datasets

The Kaetsu Coast is located on the middle north coast of Japan and faced to the Sea of Japan (Fig. 1). At Kanazawa Port on the middle of the coast, the wave observation has been carried out since the early 1970s by the NOWPHAS (Nationwide Ocean Wave information network for Ports and HArborS) project by the Ministry of Land, Infrastructure, Transport and Tourism, Japan (Nagai *et al.*, 1994). In this study, the data from January 1971 to December 2012 have been used for the analyses of wave characteristics and related properties, unless otherwise mentioned. Two types of instruments have been used for the measurements of wave characteristics:

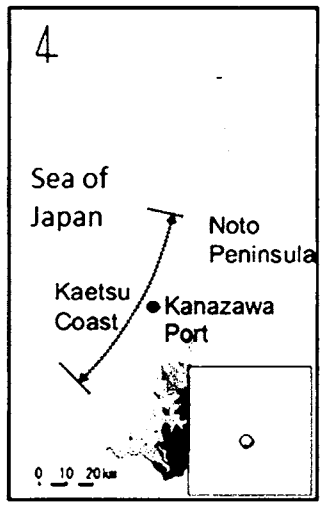

Fig. 1 Location of study area and wave observation site.

Ultrasonic-type wave gauge (USW) from January 1971 to July 2003 at the water depth of 20.2 m, and Doppler-type wave directional meter (DWDM) from August 2003 until now at 21.1 m of water depth. In both durations, the water depth at the observation site has been relatively shallow. The observation data includes mean, significant, and 1/10 wave height and period. Among them the significant wave height and period are analyzed in this study; hereafter the wave height and period indicate the significant wave height and period, respectively, unless otherwise mentioned. The statistical data processing had been performed in time intervals of 2 hours from the start of observations until 2005. From 2006, the data processing has been conducted every 20 minutes. In this study, the time intervals of 2 hours were used. The total number of original data over 4 decades is 176,064. Among them, 27,174 missing data are included, which is 15.4 % of the total data. The measurement of wave direction started from 2004.

The NOWPHAS dataset also includes the wave observation data for infragravity range. In this analysis, the infragravity waves are defined as the waves whose periods are larger than 32 s. The available data of infragravity wave measurement is limited in duration 2003-2008. It is noted that the data length of infragravity waves is less than 10 years and is not sufficiently long to obtain statistically stable results.

2) Method of Analysis

2-1) Estimation of Deep Water Wave Height

Prior to the analysis, the acquisition rate for each year as well as each month was computed as a ratio between the number of normal data and the total data. When the acquisition rate was less than 70 %, the relative year or month were omitted. In the analysis, when appropriate, the whole year was divided into 4 seasons: spring: from March to May; summer: from June to August; autumn: from September to November and winter: from December to next February.

The wave heights were first converted into corresponding deep water values based on the linear wave (shoaling) theory (*e.g.* Masselink *et al.*, 2003). According to the shoaling theory, the relationship between wave heights in deep and shallow water area can be described as:

$$\frac{H}{H_0} = K_s. \qquad (1)$$

Hereafter the subscript 0 represents for wave quantities at deep water area. K_s is the shoaling coefficient, which is defined as:

$$K_s = 1/\sqrt{\tanh kh + kh(1-\tanh^2 kh)}, \qquad (2)$$

where k is wave number and h is water depth. K_s is a function of water depth and not of wave height. In deep water K_s =1.0. It takes a minimum value of 0.91 at h/L_0 is equal to approximately 0.15 (L_0: deep water wave length). As the water depth reduces it increases without limit. Based on equation (1) and (2), the wave height in deep water area was computed by

$$H_0 = H_{obs}/K_s = H_{obs}\sqrt{\tanh kh + kh(1-\tanh^2 kh)}, \qquad (3)$$

in which H_{obs} is the observed wave height and h is water depth of the measurement.

2-2) Estimation of Potential Deep-Water Wave Energy

The wave energy flux of ocean irregular waves is given by the following equation (Takahashi and Adachi, 1989; Nagai *et al.*, 1998)

$$W = \frac{\rho g^2}{32\pi} H_{rms}^2 T, \qquad (4)$$

where W the wave energy flux per unit length of wave-crest (N or W/m), ρ the water density (1025 kg/m^3), g the acceleration by gravity (9.8 m/s^2), T the wave period (s), and H_{rms} the root-mean-square wave height (m).

If the Rayleigh distribution is assumed, the relation between H_{rms} with deep-water significant wave height H_0 becomes (*e. g.* Goda, 2010)

$$H_{rms}^2 \approx \frac{1}{2} H_0^2 . \quad (5)$$

The period of component waves is assumed to be the same as the period of significant wave in deep water (Takahashi and Adachi, 1989; Nagai *et al.*, 1998):

$$T = T_0 . \quad (6)$$

In combination of equations (4), (5), and (6), the wave energy flux per unit alongshore length (hereafter called as wave power) is elucidated as

$$W = \frac{\rho g^2}{64\pi} H_0^2 T_0 . \quad (7)$$

The averaged wave power in a given time duration (t=0 to t_0) is calculated as follows:

$$WP = \frac{1}{t_0}\int_{t=0}^{t=t_0} W dt \cong \frac{1}{t_0}\frac{\rho g^2}{64\pi}\sum_{n=1}^{N} H_{0,n}^2 T_{0,n}\Delta t , \quad (8a)$$

where the subscript n denotes the n-th value in the wave record, N is the total number of data during the given duration, and Δt is the time interval of each observation ($\Delta t = t_0/N$). In the analysis, the time intervals of statistical data processing (2 hours = 7,200 s) were used for Δt. The value of t_0 was set as the length of each month. The corresponding accumulative wave energy flux during the given duration is

$$E = WP \times t_0 = \int_{t=0}^{t=t_0} W dt \cong \frac{\rho g^2}{64\pi}\sum_{n=1}^{N} H_{0,n}^2 T_{0,n}\Delta t . \quad (8b)$$

The monthly variation and directional distribution of wave power and corresponding accumulative energy fluxes were calculated based on equations (8).

2-3) Estimation of Breaker Heights and Depths

In terms of breaking waves, the analysis combines the shoaling wave theory with the breaker height equation proposed by Keulegan and Patterson (1940) to calculate the breaker height (H_b) and depth (h_b) as:

$$H_b = \gamma h_b . \quad (9)$$

Keulegan and Patterson defined the range of the value of γ between 0.71 and 0.78. It is noted that different researchers proposed different ranges of γ; for example, Munk (1949), based on solitary wave theory, showed that γ was approximately 0.78; Thornton and Guza (1982) analyzed the result of a field measurement and determined that the coefficient γ was in the ranges from 0.3 to 1.1. This analysis used the value of 0.8 for γ.

The computation of breaker height and depth has been performed as follows: First, breaking wave heights and water depths were calculated based on the shoaling coefficient (2) and the breaking criteria (9); monthly variation of breaking wave heights and water depths were then figured out; the cumulative probability of occurrence for breaker heights p (H_b) and depths p (h_b) were estimated to deduce the seasonal variation of the width of the breaker zone. Corresponding cumulative occurrence probability (probability of non-exceedance) for breaker heights P (H_b) and depths P (h_b) were also examined.

$$P(H_b) = \int_0^{H_b} p(H_b) dH , \quad (10a)$$

$$P(h_b) = \int_0^{h_b} p(h_b) dh . \quad (10b)$$

2-4) Estimation of Closure Depths

The inner closure depth is defined as the seaward limit of significant cross-shore sediment transport by waves. On the basis of linear wave theory, Hallermeier (1981) proposed an inner closure depth formula for quartz sand in seawater as:

$$D_s = (2.28 - 10.9\frac{H_0}{L_0})H_0 , \quad (11)$$

where H_0 and L_0 are the height and length of deep water wave, respectively.

This study used equation (11) to estimate the closure depth. The seasonal variation of occurrence probability p (D_s) and the cumulative probability P (D_s) at the study area were also analyzed.

2-5) Estimation of Sunamura Index

Sunamura and Horikawa (1974) established a classification formula for shoreline changes by means of a non-dimensional parameter C, which has been known as Sunamura index as:

$$C = (H_0 / L_0)(\tan\beta)^{0.27}(d_{50} / L_0)^{-0.67}, \qquad (12)$$

in which, $\tan\beta$ is the average beach slope from the initial shoreline up to the critical water depth of sediment movement. d_{50} is the median diameter of sediment in the sea water. Sunamura (1980) eliminated non-credible data and added new data to define the demarcation value of C of 18 for field observed data between recession and advance of shoreline; when $C > 18$ the shoreline was recessed, while it was advanced when $C < 18$. This research uses the equation (12) for the estimation of Sunamura index in order to deduce the seasonal characteristics of shoreline changes at the Kaetsu Coast. The northern part of the Kaetsu coast is composed of gently sloping beach with fine sand. In this research, accordingly the values of $\tan\beta = 0.01$ and $d_{50} = 0.18$ mm were used in equation (12) as typical values for the study area.

2-6) Analysis of Infragravity Waves

Initially, the datasets of infragravity wave heights (H_L) were arranged into daily- as well as monthly-mean values. After that, the variations of the daily- and monthly-mean of infragravity wave heights were computed to clarify the seasonal variations. Then, the relation between infragravity wave heights and the variation of significant wave heights in deep water were examined to reveal the connection between them.

III. Characteristics of Wave Energy Transported by Offshore Wind Waves

The seasonal and directional variation of wave power, which is defined as the energy flux of the incoming waves per unit time and (alongshore) width, is shown in Fig. 2 (a). The corresponding directional distribution of accumulative energy flux E is described in Fig. 2 (b). In these figures WP and E indicate the averaged values over 2004-2012. Clearly, the wave power in winter is much larger than that in summer. In winter the wave power is around 20 kW/m, while it is just about 1 kW/m in summer. The values are about 6 kW/m in spring and autumn. The corresponding accumulative energy flux E is approximately 1.6×10^8 kN in winter, 8.0×10^6 kN in summer, and 5.0×10^7 kN in each of spring and autumn. The accumulative incoming wave energy flux in winter reaches 60 percent of the total energy. Generally, at Kanazawa Port, the waves approach shoreline from the SW to NNE direction. The annual mean of wave power coming from all of the directions is about 8.2 kW/m. The corresponding annual energy flux is 2.6×10^8 kN. Among them, the WNW, NW, and NNW are the dominant directions of wave incidence in which the wave energies

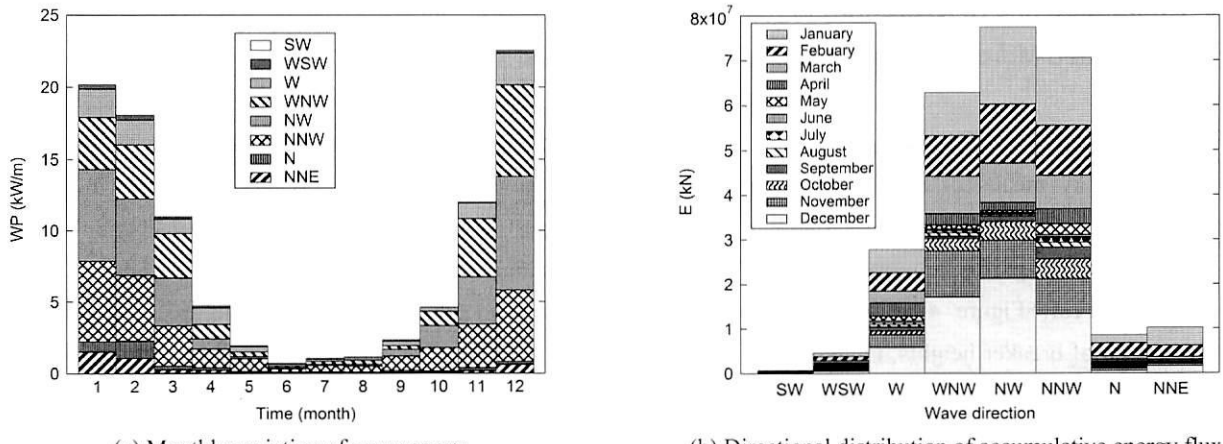

(a) Monthly variation of wave power (b) Directional distribution of accumulative energy flux

Fig. 2 The distribution of incoming wave energy in duration 2004-2012 (left: Monthly variation of wave power, right: Directional distribution of accumulative energy flux) .

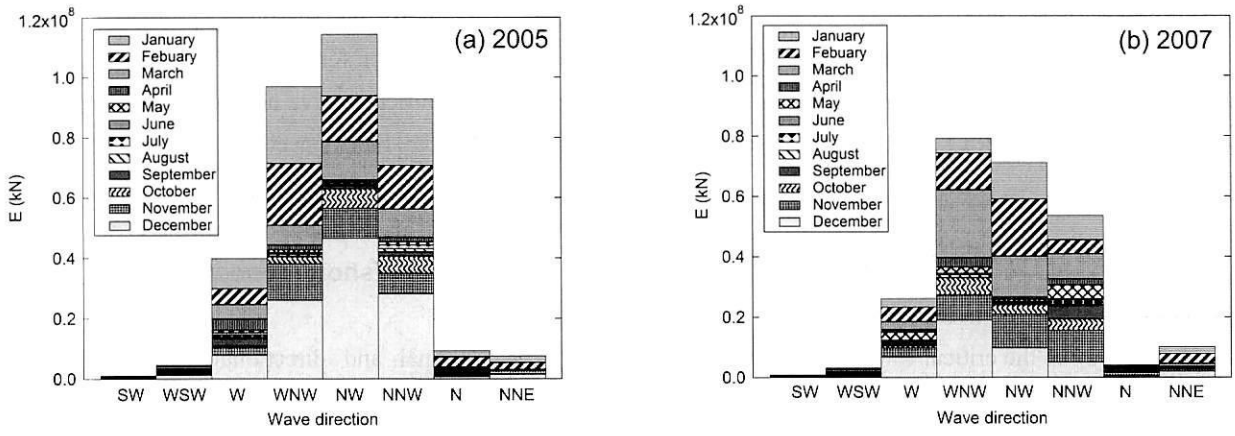

Fig. 3 The directional distribution of accumulative wave energy flux in two typical years.

are concentrated. The annual-mean wave power from these dominant directions is 6.6 kW/m and corresponding accumulative wave energy (2.1×10^8 kN) reaches 80 % of the total. It is noted that these dominant directions of wave energy incidence represent the dominant wave direction in winter season.

Next, the year to year variation of wave power was examined. Figure 3 shows the directional distribution of accumulative energy flux in two typical years. In 2005 the total wave energy flux over a whole year was the highest (E=3.6×10^8 kN) and in 2007 it was the lowest (E=2.5×10^8 kN). In 2005 the annual mean of wave power is about 11.4 kW/m and the dominant direction of incoming waves is the NW. In 2007 the annual mean of wave power is approximately 7.7 kW/m and the dominant direction of waves slightly moves to the WNW.

IV. Characteristics of Nearshore Waves and Related Morphological Indices

1) Breaker Heights and Depths

The monthly means of the breaker heights were investigated to examine the seasonal variation of breaker zone width where significant morphological change is expected to occur. Figure 4 shows the variation in monthly-mean of breaker heights, including the average, maximum, and minimum values in duration 1971-2012. These figures clearly illustrate that the breaker heights are the highest in winter, medium in spring and autumn and the lowest in summer. The average values of breaker

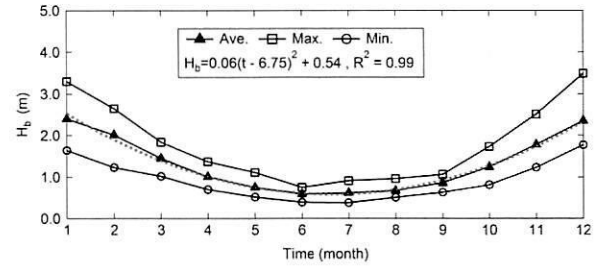

Fig. 4 Seasonal variation of monthly-mean breaker height in duration 1971-2012.

heights in summer are around 0.6 m, while they are greater than 2.0 m in winter. In spring and autumn, breaking wave height is in the range 0.6 to 2.0 m. In addition, the mean values correlate very well with the following second order polynomial with a high correlation coefficient (R^2 = 0.99).

$$H_b = 0.06(t\text{-}6.75)^2 + 0.54. \quad (13)$$

The seasonal variation of breaker depths at the breaking points is quite similar to breaker height variation as shown in Fig. 5. The breaker depths in winter are the deepest with the mean values approximately 3.0 m, while in summer they are the shallowest, around 0.8 m. In spring and autumn, the water depths are in the range 1.0 m to 2.0 m. Moreover, the mean values correlate very well with the following second order polynomial, in which the correlation coefficient is similar to that of average breaker height (R^2 = 0.99).

$$h_b = 0.076(t\text{-}6.64)^2 + 0.68. \quad (14)$$

The maximum and minimum values of monthly-mean of breaker height and depth indicate essentially the same patterns of variation. The strength of year-to-year variation in the same month can be inspected from the range of the data, which is defined as the difference between the maximum and minimum values. The figures clearly show that the range of both breaker height and breaker depth become larger in winter and smaller in summer. In the study duration, the maximum values of monthly-mean breaker heights and depth are approximately 3.5 m and 4.3 m, respectively.

Next, the cumulative occurrence probability of breaker depth $P(h_b)$ is investigated in duration 1971-2012 for each season. According to Fig. 6, in winter season 80 percent of waves break at the area with water depths less than approximately 4.0 m, while in summer this value is just approximately 1.0 m. Namely, in summer the waves break only in the narrow area very close to the shoreline. In the spring and autumn the corresponding water depth is around 2.0 to 2.5 m.

Figure 7 indicates the monthly variation of cumulative occurrence probability of breaker depth in duration 1971-2012. In winter season 10 to 20 percent of waves break at the breaker depths larger than 4.5 m. In summer, the waves do not break at the water depth more than 2.5 m. In spring and autumn the waves break at water areas shallower than 5.5 m. These results indicate that the cross-shore width of surf zone where intensive morphological changes occur is substantially variable in time at the Kaetsu Coast.

2) Closure Depths

The cumulative occurrence probability of inner closure depths $P(D_s)$ in duration 1971-2012 at Kanazawa are shown for each season in Fig. 8. In winter season, the closure depths are estimated to be less than 6.0 m approximately 80 % of time. In contrast, in summer season, the closure depths are less than 2.0 m more than 80 % of time. In spring and autumn, the closure depths are around 3.0 m about 80 % of time.

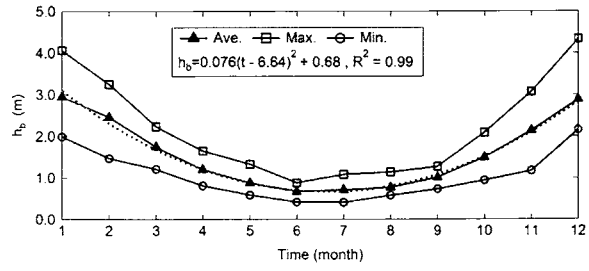

Fig. 5 Seasonal variation of monthly-mean breaker depth in duration 1971-2012.

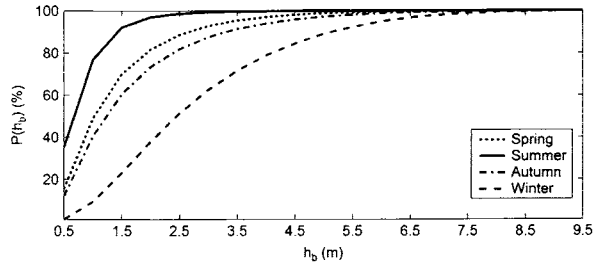

Fig. 6 The cumulative probability distribution of breaker depth in duration 1971-2012.

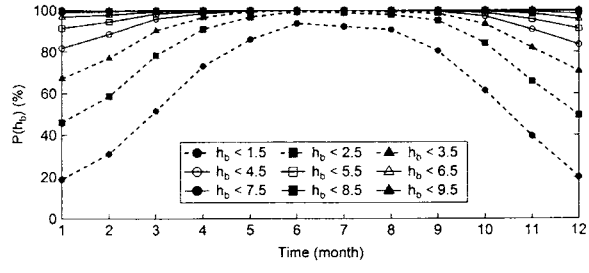

Fig. 7 The cumulative probability of breaker depth in duration 1971-2012.

Next, the monthly variation of cumulative occurrence probability of inner closure depth is examined in Fig. 9. The figure illustrates that in winter season the inner closure depths are mostly less than 10.0 m. In summer, 4.0 m seems to be the limitation of closure depths. In spring and autumn, most of closure depths are less than 7.0 m.

3) Sunamura Index

Figure 10 demonstrates the monthly variation of Sunamura index averaged over the study duration 1971-2012. The corresponding minimum and maximum values in the same duration are also included in the figure for comparison. The figure clearly illustrates that the

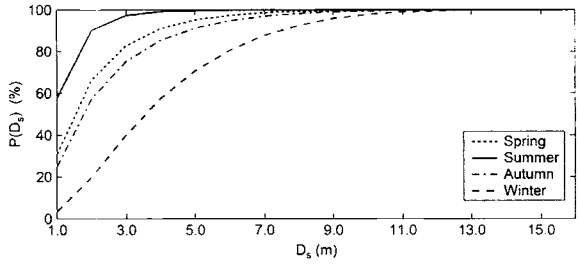

Fig. 8 The cumulative probability of inner closure depths in duration 1971-2012.

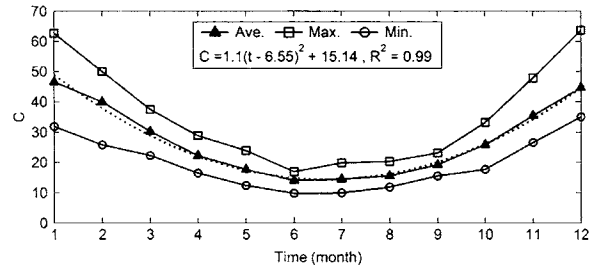

Fig. 10 The monthly variation of Sunamura index in duration 1971-2012.

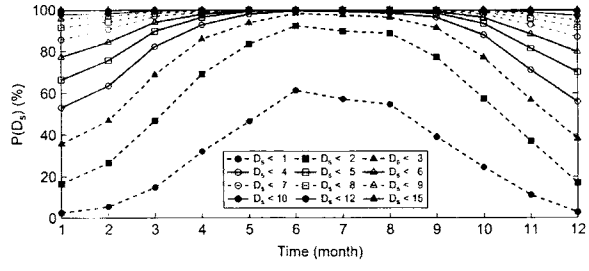

Fig. 9 The monthly variation of cumulative probability of inner closure depths in duration 1971-2012.

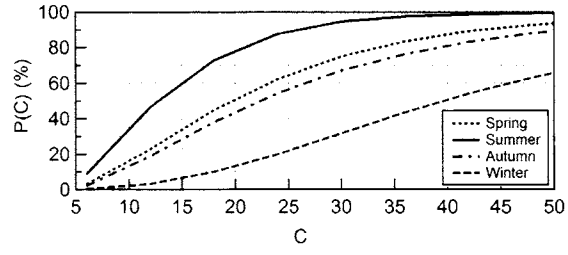

Fig. 11 The cumulative probability of Sunamura index in duration 1971-2012.

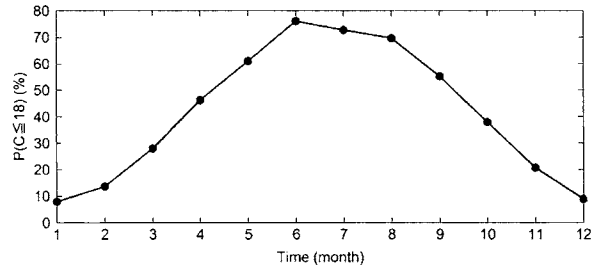

Fig. 12 The monthly variation of probability for waves with C<=18 in duration 1971-2012.

values of Sunamura indices are the lowest in summer; the averaged value is around 15. In contrast, in winter these indices are the highest with the averaged values larger than 40. In spring and autumn these indices are the medium, in which the values are in the range 18 to 35. Referring to the demarcation value of Sunamura index (C=18), it is deduced that the shoreline is advanced during summer and the recessions of shoreline generally occur in other seasons. The transitions from recessions to advances of the shoreline are inferred to occur in March, from advances to recessions in September. In addition, the monthly-mean values of Sunamura indices averaged over study duration correlate very well with the following second order polynomial with a high correlation coefficient (R^2 = 0.99).

$$C = 1.1(t\text{-}6.55)^2 + 15.14. \quad (15)$$

Next, the cumulative occurrence probability of Sunamura index P (C) is examined for each season in Fig. 11. It shows that in winter most of waves induce recession of the shoreline, in which the percentage for C > 18 reaches around 90 %. In contrast, the majority of waves in summer have a role to advance the shoreline. In this season C is less than the threshold value over 70 % of time. In spring and autumn, approximately 50 to 60 percent of waves induce shoreline recession and 50 to 40 percent make the shoreline advance, respectively.

Next, the monthly variation of occurrence probability corresponding to shoreline advance P (C<=18) was rearranged and plotted in Fig. 12. According to the figure, in June the percentage of Sunamura indices less than 18 is approximately 80 percent of time. This is ten times higher than that in January or December which is just 8 percent. In spring and autumn the rate of change in P (C<=18) is large. The probability exceeds 50 percent from May to September. From these results it is deduced

that the dominant direction of cross-shore sediment transport is landward during May to September, while it alternates to seaward during October to next March. In April, where P (C<=18) is approximately 50 %, the net amount of sediment transport in the cross-shore direction is inferred to be small.

V. Characteristics of Infragravity Waves

1) Seasonal Variation

The variation of infragravity waves also has significant seasonal changes like that of wind waves. Figure 13 describes the seasonal variation of monthly-mean height of infragravity waves (H_L) observed at Kanazawa Port year by year (Fig.13 (a)) and the corresponding averaged values (Fig.13 (b)) in duration 2003-2008. Infragravity waves are the highest in winter, the smallest in summer and the medium in spring and autumn. The monthly-mean heights averaged over the duration are around 0.030 m in summer, while in winter they are around 0.100 m. The standard deviations were also examined to investigate the scatter of data. The standard deviations in summer are less than 0.01 m, while they are 0.02 to 0.03 m in winter. In the figure, the maximum and minimum values in the same duration are also included. The maximum values of the monthly-mean heights during the observation period are approximately 0.035 and 0.130 m in summer and winter, respectively. The minimum values are around 0.025 m in summer and 0.080 m in winter. The monthly variation of infragravity wave heights in duration 2003 to 2008 can be approximated very well by the following second order polynomial with a correlation coefficient of R^2=0.97.

$$H_L = 0.003(t - 5.67)^2 + 0.046. \quad (16)$$

2) Relation with Wind Waves

Next, the relation between daily-mean of significant wave heights and infragravity wave height are compared in two typical years (Fig. 14). The figures clearly illustrate that patterns of the daily variation of both wind waves and infragravity waves are quite the same.

Figure 15 compares the seasonal variation of monthly-mean of infragravity wave heights and significant wind wave heights. The figure illustrates that the pattern of these variations are quite the same. The

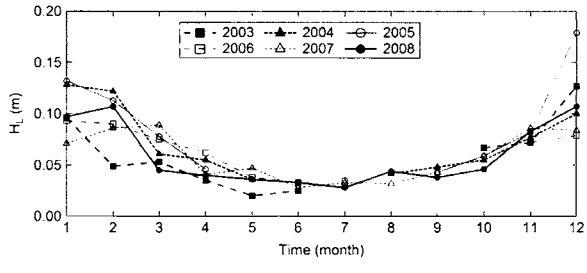

(a) Year by year values

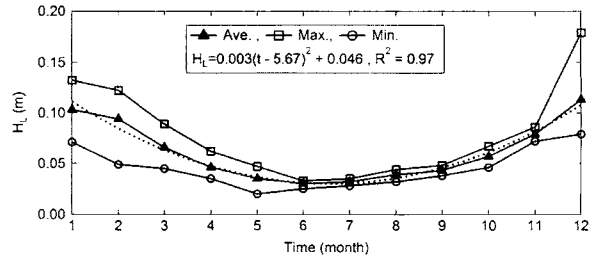

(b) Avarage, maximum and minimum values in duration 2003-2008

Fig. 13 Seasonal variation of monthly-mean height of infragravity waves (upper: Year by year values, lower: Avarage, maximum and minimum values in duration 2003-2008).

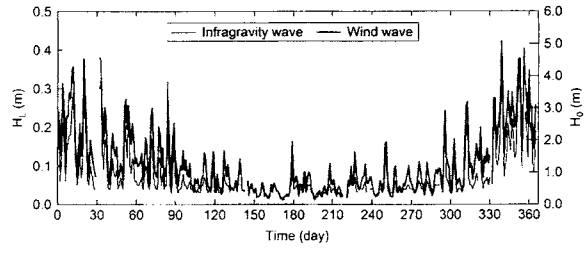

(a) 2005

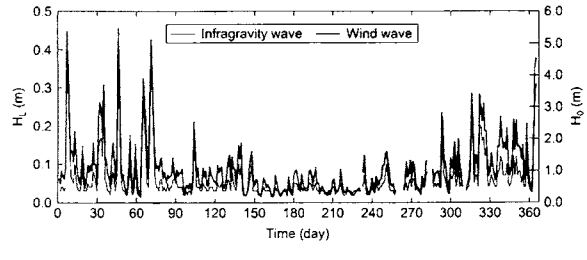

(b) 2007

Fig. 14 Comparison of the temporal variation of daily-mean heights of infragravity and wind wave (upper: 2005, lower: 2007).

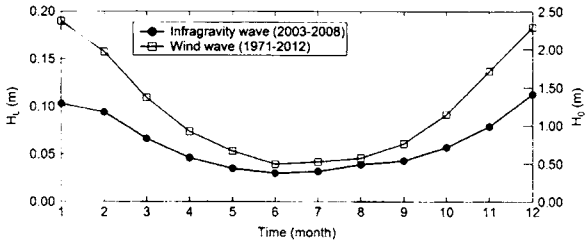

Fig. 15 Comparison of monthly-mean height of infragravity and wind wave.

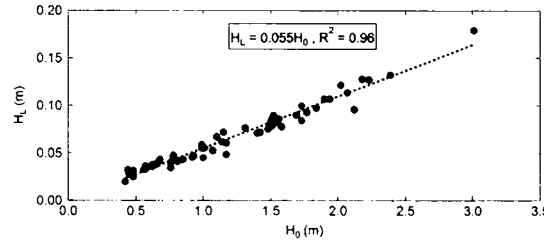

Fig. 16 Relation between monthly-mean wind wave height and infragravity wave height in duration 2003-2008.

relation between monthly significant wind waves and infragravity wave heights at Kanazawa in duration 2003-2008 is shown in Fig. 16. The heights of infragravity waves and wind waves at this site can be linearly correlated very well by the following equation

$$H_L = 0.055H_0 , \qquad (17)$$

in which the correlation coefficient is very high (R^2 = 0.96). On average, the infragravity wave height is approximately 5.5 % of significant wind wave height.

VI. Summary Remarks

This study investigated the wave data obtained at Kanazawa Port in duration 1971-2012 in order to clarify the characteristics of deep-water wave energy flux, breaking wave properties (breaker height and depth) in the nearshore, and infragravity waves. In addition, the related morphological parameters (closure depth and Sunamura index) are estimated to deduce the possible influence of wave forcing on the morphological change at the Kaetsu Coast. The seasonal variation of wave energy flux indicated that most of the wave energy is transported during winter season. The directional distribution showed that approximately 80 % of total wave energy incident the coast from the WNW, NW, and NNW direction. The pattern of seasonal variation of breaker height and depth are quite similar. The values are the highest in winter, medium in spring and autumn and the lowest in summer. The cumulative probability distribution of breaker depth indicated that in winter 80 % of waves break at the area with water depths less than 4.0 m, while in summer this water depth is just approximately 1.0 m. In the spring and autumn the water depth of the area at which 80 % of waves break is less than 2.5 m. The cumulative probability of closure depth revealed that over 80 % of time the closure depths are less than 6.0 m in winter, 2.0 m in summer, 3.0 m in spring and autumn. Similar to breaking properties, the monthly mean of Sunamura indices are the lowest in summer, the highest in winter season, and medium in spring and autumn. It was deduced that during summer season the shoreline is advanced and the recessions of shoreline generally occur in other seasons. The transitions from recessions to advances of the shoreline occur in March, from advances to recessions in September. Infragravity waves have the same seasonal pattern with the wind waves. The patterns of the daily as well as monthly variation of infragravity waves are similar to that of wind waves. The heights of infragravity waves and wind waves can be linearly correlated very well.

Acknowledgment: This study was partially supported by a Grant-in-Aid for Scientific Research by the Japan Society for the Promotion of Science (No.16K06505).

References

Goda, Y., 2010: *Random seas and design of maritime structures.* 3rd Edition, World Scientific, Singapore, 708p.

Guza, R. T. and Thornton, E. B., 1982: Swash oscillations on a natural beach. *Journal of Geophysical. Research*, **87**, 483-491.

Hallermeier, R. J., 1981: A profile zonation for seasonal sand beaches from wave climate. *Coastal Engineering*, **4**, 253-277.

Keulegan, G. H. and Patterson, G. W., 1940: Mathematical

theory of irrotational translation waves. *Journal of Research of the National Bureau of Standards,* **24**, 48-100

Kobune, K., Sugawara, K. and Goto, C., 1988: Wave climate along the coast of Japan. *Proceedings of Japan Conference on Coastal Engineering*, **35**, 232-236 (in Japanese).

Masselink, G., Hughes, M. G. and Knight, J., 2003: *Introduction to coastal processes and geomorphology.* Hodder Education, London, 354p.

Munk, W. H., 1949: The solitary wave theory and its application to surf problems. *Annals of the New York Academy of Sciences*, **51**, 376-462.

Nagai, T., 1997: Study on Japanese coastal wave characteristics obtained from the NOWPHAS wave observation network. *Technical Note of the Port and Harbour Research Institute, Ministry of Transport, Japan*, **863**, p113.

Nagai, T., Sugahara, K., Hashimoto, N., Asai, T., Higashiyama, S. and Toda, K., 1994: Introduction of Japanese NOWPHAS system and its recent topics. *Proceedings of the International Conference on Hydro-Technical Engineering for Port and Harbor Construction (HYDRO-PORT'94), PHRI*, 67-82.

Nagai, T., Watanabe, H. and Kawaguchi, K., 1998: Characteristics of wave power around Japan based on long term coastal wave observation data. *Technical Note of the Port and Harbour Research Institute, Ministry of Transport Japan*, **895**, 1-26 (in Japanese).

Nguyen, T. C. and Yuhi, M., 2015: Long-term variation of wave characteristics on the Kaetsu Coast, Japan. *Journal of Japan Society of Civil Engineers, Ser. B3 (Ocean Engineering)*, **71**, I_359-I_364.

Nguyen, T. C., Yuhi, M. and Ueno, T., 2016: Comparisons of regional wave climate along the Sea of Japan Coast. *Japan Sea Research*, **47**, 9-28.

Seki, K., Kawai, H. and Satoh, M., 2011: Long-term variability of wave characteristics around the Japanese coasts. *Journal of Japan Society of Civil Engineers, Ser. B3 (Ocean Engineering)*, **67**, I_1-I_6 (in Japanese).

Seki, K., Kawai, H., Kawaguchi, K. and Satoh, M., 2012: Long-term trend of wave characteristics on Japanese coast based on NOWPHAS data. *Proceedings of the 22nd International Offshore and Polar Engineering Conference,* 685-692.

Shimizu, K., Nagai, T., Satomi, S., Lee, J. H., Tomita, Y., Kudaka, M. and Nukada, K., 2006: Long-term wave climate study based on meteorological and observed wave data. *Annual Journal of Coastal Engineering, JSCE*, **53**, 131-135 (in Japanese).

Sunamura, T., 1980: Predictive model for shoreline-position change on natural beaches. *Proceedings of the 27th Japanese Conference on Coastal Engineering, JSCE*, 255-259 (in Japanese).

Sunamura, T. and K. Horikawa., 1974: Two-dimensional beach transformation due to waves. *Proceedings of the 14th International Conference on Coastal Engineering*, 920-938.

Takahashi, S. and Adachi, T., 1989: Wave power around Japan from a viewpoint of its utilization. *Technical Note of the Port and Harbour Research Institute, Ministry of Transport Japan*, **654**, 1-18 (in Japanese).

Thornton, E. B. and Guza, R. T., 1982: Energy saturation and phase speeds measured on a natural beach, *J. Geophys. Res*, **87**, 9499-9508.

Yamaguchi, M., Ohfuku, M., Hatada, Y., Nonaka, H. and Emoto, K., 2007: Analyses of year-to-year variation and trend for wave climatic parameters along the coasts of Japan using long-term measurement data. *Proceedings of Coastal Engineering, JSCE*, **54**, 1296-1300 (in Japanese).

石川県加越海岸における波浪特性および関連する地形変化指標の季節変動

NGUYEN Trinh Chung[1]・由比政年[2*]・上野卓也[3]

2016年9月23日受付
2016年12月1日受理

要　旨

本研究では，金沢港において1971～2012年に取得された波浪観測データに基づいて，石川県加越海岸における波浪および地形変化指標の季節変動特性の解析を行った。まず，入射する波エネルギーの季節変動と方向分布を解析した。来襲する波エネルギーの大部分は冬季に集中し，支配的入射方向は，西北西，北西，北北西である。次に，砕波波高・水深，移動限界水深，および，汀線変化指標（砂村パラメータ）の季節変動を算定した。これらのパラメータの変動傾向は共通であり，冬季に最大，夏季に最小，春季・秋季に中間的な値を取る。砕波水深および移動限界水深の発生確率は顕著な季節変動を示し，有意な地形変動が生じる水深域は季節により大きく変動することが示唆された。砂村パラメータの変動は，汀線は夏季に前進，それ以外の季節では後退傾向にあることを示した。汀線が後退から前進に，前進から後退に転じる時期はそれぞれ3月，9月と推定された。最後に，長周期波の波高変化について検討を行った。長周期波高の変動は風波波高の変動に良く追随し，同様の変動特性を示すこと，また，両者は線形の関係式で良く関係づけられることを示した。

キーワード：加越海岸，波候，季節変動，波エネルギー，地形変動指標

[1]金沢大学大学院自然科学研究科博士後期課程環境科学専攻　〒920-1192 金沢市角間町
[2]金沢大学理工研究域環境デザイン学系　〒920-1192 金沢市角間町
[3]金沢大学大学院自然科学研究科博士前期課程環境デザイン学専攻　〒920-1192 金沢市角間町
*連絡著者